

Heat transport in RbFe₂As₂ single crystal: evidence for nodal superconducting gap

Z. Zhang,¹ A. F. Wang,² X. C. Hong,¹ J. Zhang,¹ B. Y. Pan,¹
J. Pan,¹ Y. Xu,¹ X. G. Luo,^{2,3} X. H. Chen,^{2,3} and S. Y. Li^{1,3,*}

¹State Key Laboratory of Surface Physics, Department of Physics,
and Laboratory of Advanced Materials, Fudan University, Shanghai 200433, P. R. China

²Hefei National Laboratory for Physical Science at Microscale and Department of Physics,
University of Science and Technology of China, Hefei, Anhui 230026, P. R. China

³Collaborative Innovation Center of Advanced Microstructures, Nanjing 210093, P. R. China

(Dated: May 10, 2019)

The in-plane thermal conductivity of iron-based superconductor RbFe₂As₂ single crystal ($T_c \approx 2.1$ K) was measured down to 100 mK. In zero field, the observation of a significant residual linear term $\kappa_0/T = 0.65$ mW K⁻² cm⁻¹ provides clear evidence for nodal superconducting gap. The field dependence of κ_0/T is similar to that of its sister compound CsFe₂As₂ with comparable residual resistivity ρ_0 , and lies between the dirty and clean KFe₂As₂. These results suggest that the (K,Rb,Cs)Fe₂As₂ serial superconductors have a common nodal gap structure.

PACS numbers: 74.70.Xa, 74.25.fc

I. INTRODUCTION

The iron-based superconductors [1, 2] have attracted great attention since Hosono and co-workers reported the discovery of 26 K superconductivity in fluorine doped LaFeAsO in 2008 [1]. Unfortunately, there is still no consensus on the superconducting mechanism in them, mainly due to their complicated electronic structures [3–5].

There are many families of the iron-based superconductors, such as LaO_{1-x}F_xFeAs (“1111”), Ba_{1-x}K_xFe₂As₂ (“122”), NaFe_{1-x}Co_xAs (“111”), and FeSe_xTe_{1-x} (“11”) [6]. Among them, the “122” family is the most studied one due to the easy growth of sizable high-quality single crystals [7]. Intriguingly, the members of this family do not share a universal superconducting gap structure. While the optimally doped Ba_{0.6}K_{0.4}Fe₂As₂ and BaFe_{1.85}Co_{0.15}As₂ have nodeless superconducting gaps [4, 8–10], the extremely hole-doped KFe₂As₂ was reported to be a nodal superconductor [11, 12]. Furthermore, the isovalently doped BaFe₂(As_{1-x}P_x)₂ [13–15] and Ba(Fe_{1-x}Ru_x)₂As₂ [16] also manifest nodal superconductivity. So far, the origin of these nodal superconducting gaps is still under debate, particularly in KFe₂As₂ [11, 12, 17–19]. The detailed thermal conductivity study provided compelling evidences for a *d*-wave gap in KFe₂As₂ [17], but the low-temperature angle-resolved photoemission spectroscopy (ARPES) measurements clearly showed nodal *s*-wave gap [19]. Recent ARPES and thermal conductivity experiments on highly hole-doped Ba_{1-x}K_xFe₂As₂ also support nodal *s*-wave gap [20, 21].

KFe₂As₂ has two sister compounds, CsFe₂As₂ and RbFe₂As₂, and both of them are superconducting [22, 23]. While muon-spin spectroscopy measurements on RbFe₂As₂ polycrystals suggested that RbFe₂As₂ is best described by a two-gap *s*-wave model [24, 25], recent specific heat and thermal conductivity measurements on CsFe₂As₂ single crystals provided clear evidences for

nodal superconducting gap in CsFe₂As₂ [26, 27]. To clarify whether the superconducting gap structure of RbFe₂As₂ is indeed different from those of KFe₂As₂ and CsFe₂As₂, more experiments on RbFe₂As₂ single crystals are highly desired.

In this paper, we present the low-temperature thermal conductivity of RbFe₂As₂ single crystal down to 100 mK. A significant residual linear term $\kappa_0/T = 0.65 \pm 0.03$ mW K⁻² cm⁻¹ is obtained in zero magnetic field, and the field dependence of κ_0/T mimics that of CsFe₂As₂. These results clarify that RbFe₂As₂ is also a nodal superconductor. The three compounds KFe₂As₂, RbFe₂As₂, and CsFe₂As₂ may have a common superconducting gap structure.

II. EXPERIMENT

The RbFe₂As₂ single crystals were grown by self-flux method for the first time, and the process is the same as the growth of CsFe₂As₂ single crystals [26]. The dc magnetization was measured using a superconducting quantum interference device (MPMS, Quantum design). The specific heat measurement above 1.9 K was performed in a physical property measurement system (PPMS, Quantum design) via the relaxation method, and below 1.9 K it was measured in a small dilution refrigerator integrated into the PPMS. For transport measurements, the RbFe₂As₂ single crystal was cleaved to a rectangular shape of dimensions 2.2×1.0 mm² in the *ab* plane, with 40 μ m thickness along the *c* axis. Contacts were made directly on the sample surfaces with silver paint (Dupont 4929N), which were used for both resistivity and thermal conductivity measurements. To avoid degradation, the sample was exposed in air for less than 2 hours. The contacts are metallic with a typical resistance 100 m Ω at 2 K. In-plane thermal conductivity was measured in a dilution refrigerator, using a standard four-wire steady-state method with two RuO₂ chip thermometers, calibrated *in*

situ against a reference RuO₂ thermometer. Magnetic fields were applied along the *c* axis and perpendicular to the heat current. To ensure a homogeneous field distribution in the sample, all fields were applied at a temperature above T_c for transport measurements.

III. RESULTS AND DISCUSSION

Figure 1(a) shows the low-temperature dc magnetization of RbFe₂As₂ single crystal, measured in $H = 20$ Oe along *c* axis, with zero-field cooling process. The $T_c \approx 2.10$ K is defined at the onset of the diamagnetic transition. The magnetization does not saturate down to 1.8 K, where the superconducting volume fraction is already as large as 40%. With decreasing temperature, the superconducting volume fraction should further increase to reach the fully shielded state.

In Fig. 1(b), we present the low-temperature specific heat of RbFe₂As₂ single crystal down to 100 mK in zero field, plotted as C/T vs T . A significant jump due to the superconducting transition is observed at $T_c \approx 2.1$ K, which indicates the high quality of our sample. In order to determine the zero-field normal-state Sommerfeld coefficient γ_N , the specific heat above T_c is fitted to $C_{normal} = \gamma_N T + \beta T^3 + \eta T^5$, with β and η as the lattice coefficients. The solid line in Fig. 1(b) is the best fit of C/T from 2.4 to 10 K, which gives $\gamma_N = 127.3 \pm 0.9$ mJ mol⁻¹ K⁻², $\beta = 0.66 \pm 0.04$ mJ mol⁻¹ K⁻⁴, and $\eta = 0.0029 \pm 0.0005$ mJ mol⁻¹ K⁻⁶. From the relation $\theta_D = (12\pi^4 RZ / 5\beta)^{1/3}$, where R is the molar gas constant and $Z = 5$ is the total number of atoms in one unit cell, the Debye temperature $\theta_D = 245$ K is estimated. This value is comparable to those of KFe₂As₂ and CsFe₂As₂ [26, 28].

The in-plane resistivity of RbFe₂As₂ single crystal in zero field is plotted in Fig. 1(c). The $T_c \approx 2.13$ K, defined by $\rho = 0$, agrees well with the magnetization and specific heat measurements. For the polycrystalline sample of RbFe₂As₂, $T_c = 2.6$ K was defined at the onset of the diamagnetic transition [23], which is 0.5 K higher than our single crystal. Similarly, $T_c = 2.2$ K was defined at the onset of the diamagnetic transition for the CsFe₂As₂ polycrystal [22], but $T_c = 1.8$ K was found in the CsFe₂As₂ single crystal [26]. It is unclear why the T_c shows difference between polycrystalline sample and single crystal for RbFe₂As₂ and CsFe₂As₂. In case that the single crystals have intrinsic T_c , the T_c of (K, Rb, Cs)Fe₂As₂ series (3.8, 2.1, and 1.8 K, respectively) decreases with the increase of the ionic radius of alkali metal. In the inset of Fig. 1(c), the normal-state $\rho(T)$ below 9 K can be well fitted by $\rho = \rho_0 + AT^{1.5}$, with $\rho_0 = 1.84 \pm 0.01$ $\mu\Omega$ cm and $A = 0.16$ $\mu\Omega$ cm K^{-1.5}. Similar non-Fermi-liquid behavior of $\rho(T)$ was also observed in KFe₂As₂ and CsFe₂As₂ [11, 17, 27], which may result from antiferromagnetic spin fluctuations [29]. The residual resistivity ratio RRR = $\rho(292\text{K})/\rho_0 \approx 310$ again reflects the high quality of our RbFe₂As₂ single crystal.

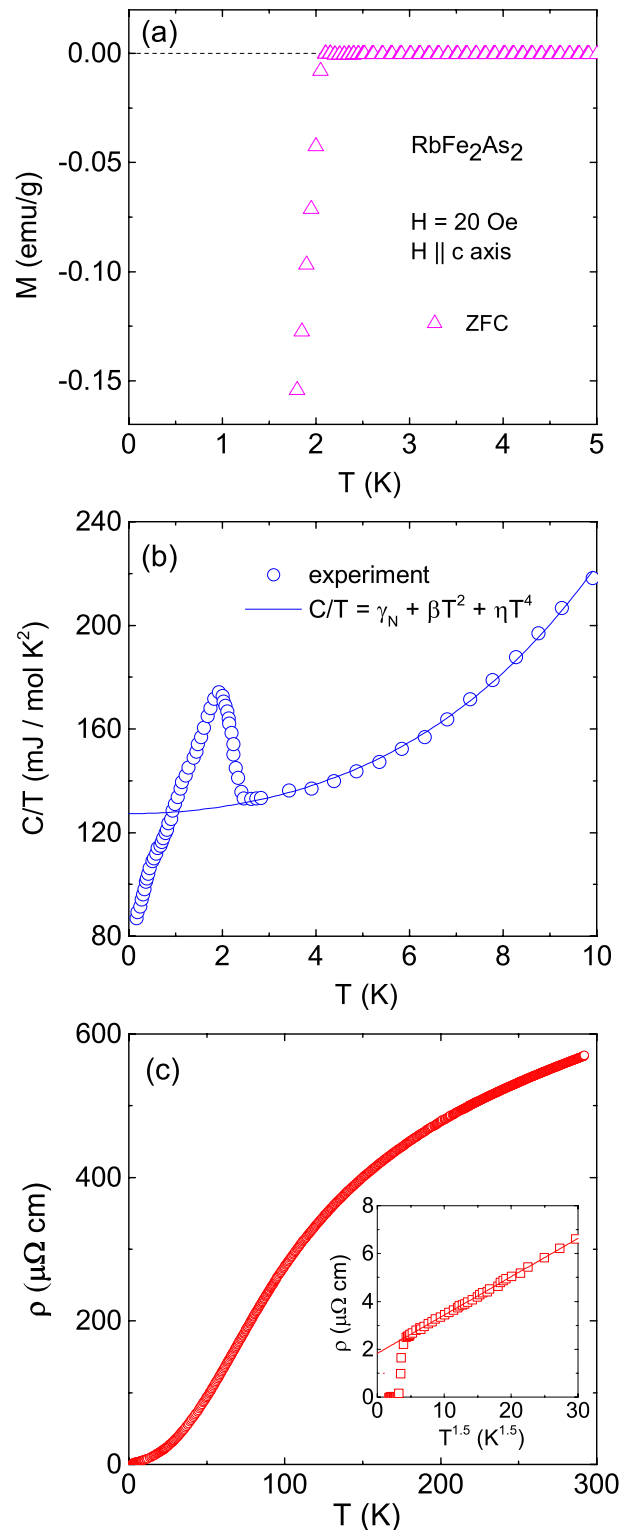


FIG. 1. (Color online). (a) Low-temperature dc magnetization of RbFe₂As₂ single crystal in $H = 20$ Oe along *c* axis, with zero-field cooling process. (b) Temperature dependence of specific heat C/T for RbFe₂As₂ single crystal in zero field, plotted as C/T vs T . The solid line is the best fit to $C_{normal} = \gamma_N T + \beta T^3 + \eta T^5$ from 2.4 to 10 K. (c) In-plane resistivity of RbFe₂As₂ single crystal in zero field. The data between 2.2 and 9 K can be fitted to $\rho = \rho_0 + AT^{1.5}$, as shown in the inset, which gives $\rho_0 = 1.84$ $\mu\Omega$ cm.

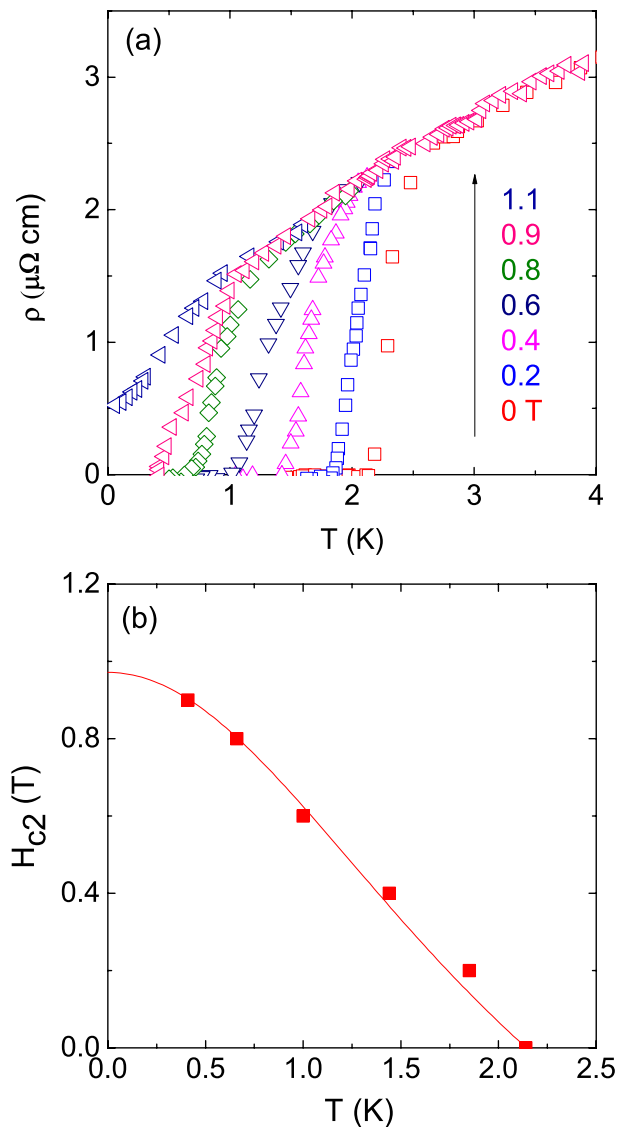


FIG. 2. (Color online). (a) Low-temperature resistivity of RbFe₂As₂ single crystal in magnetic fields up to 1.1 T. (b) Temperature dependence of the upper critical field $H_{c2}(T)$, defined by $\rho = 0$ in (a). The solid line is a fit of $H_{c2}(T)$ to the Ginzburg-Landau equation, which gives $H_{c2}(0) \approx 0.97$ T.

Figure 2(a) shows the low-temperature resistivity of RbFe₂As₂ single crystal in magnetic fields up to 1.1 T. In order to estimate the zero-temperature upper critical field $H_{c2}(0)$, the temperature dependence of $H_{c2}(T)$ is plotted in Fig. 2(b), defined by $\rho = 0$ in Fig. 2(a). $H_{c2}(0) \approx 0.97$ T is obtained by fitting the data with the Ginzburg-Landau equation $H_{c2}(T) = H_{c2}(0)[1 - (T/T_c)^2]/[1 + (T/T_c)^2]$ [30, 31].

The low-temperature heat transport measurement is a bulk technique to probe the gap structure of superconductors [32]. In Fig. 3, the in-plane thermal conductivity of RbFe₂As₂ single crystal in zero and applied field is plotted as κ/T vs T [33, 34]. The thermal conductivity at very low temperature can be usually fitted to

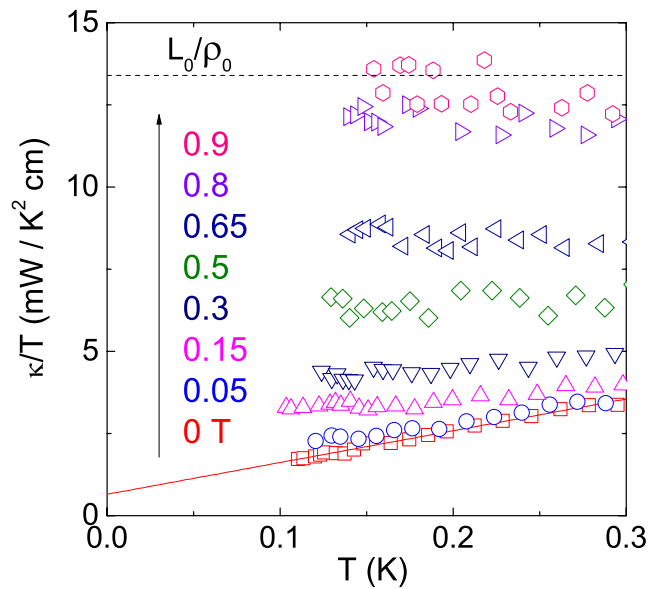


FIG. 3. (Color online). Low-temperature in-plane thermal conductivity of RbFe₂As₂ single crystal in zero and magnetic fields applied along the c axis. The solid line is a fit of the zero-field data between 0.1 and 0.3 K to $\kappa/T = a + bT$, giving a residual linear term $\kappa_0/T = 0.65 \pm 0.03$ mW K⁻² cm⁻¹. The dashed line is the normal-state Wiedemann-Franz law expectation L_0/ρ_0 , with L_0 the Lorenz number 2.45×10^{-8} W Ω K⁻² and $\rho_0 = 1.84$ μΩ cm.

$\kappa/T = a + bT^{\alpha-1}$, in which the two terms aT and bT^{α} represent contributions from electrons and phonons, respectively. The power α is typically between 2 and 3, due to specular reflections of phonons at the boundary [33, 34]. Since all the curves in Fig. 3 are roughly linear, we fix α to 2. The value $\alpha \approx 2$ has been previously observed in dirty KFe₂As₂ [11], Ba(Fe_{1-x}Ru_x)₂As₂ [16], and CsFe₂As₂ single crystals [27]. Here, we only focus on the electronic term.

In zero field, the fitting of the data between 0.1 to 0.3 K gives $\kappa_0/T = 0.65 \pm 0.03$ mW K⁻² cm⁻¹. If we slightly change the fitting range, we obtain $\kappa_0/T = 0.62 \pm 0.03$ mW K⁻² cm⁻¹ for the range below 0.27 K and $\kappa_0/T = 0.63 \pm 0.04$ mW K⁻² cm⁻¹ for the range below 0.24 K. Therefore, the value of κ_0/T basically does not depend on the temperature range chosen for the fit. Such a significant κ_0/T is usually contributed by nodal quasiparticles, thus it is a strong evidence for nodal superconducting gap [32]. Previously, $\kappa_0/T = 2.27 \pm 0.02$ and 3.6 ± 0.5 mW K⁻² cm⁻¹ were observed for dirty and clean KFe₂As₂ single crystals, respectively [11, 17]. For CsFe₂As₂ single crystal with $\rho_0 = 1.80$ μΩ cm, $\kappa_0/T = 1.27 \pm 0.04$ mW K⁻² cm⁻¹ was found [27]. The zero-field value of κ_0/T for RbFe₂As₂ is about 5% of the normal-state Wiedemann-Franz law expectation $\kappa_{N0}/T = L_0/\rho_0 = 13.5$ mW K⁻² cm⁻¹, with L_0 the Lorenz number 2.45×10^{-8} W Ω K⁻² and $\rho_0 = 1.84$ μΩ cm. In $H = 0.9$ T, the experimental data roughly satisfy the Wiedemann-Franz law, so we take 0.9 T as the bulk $H_{c2}(0)$. This

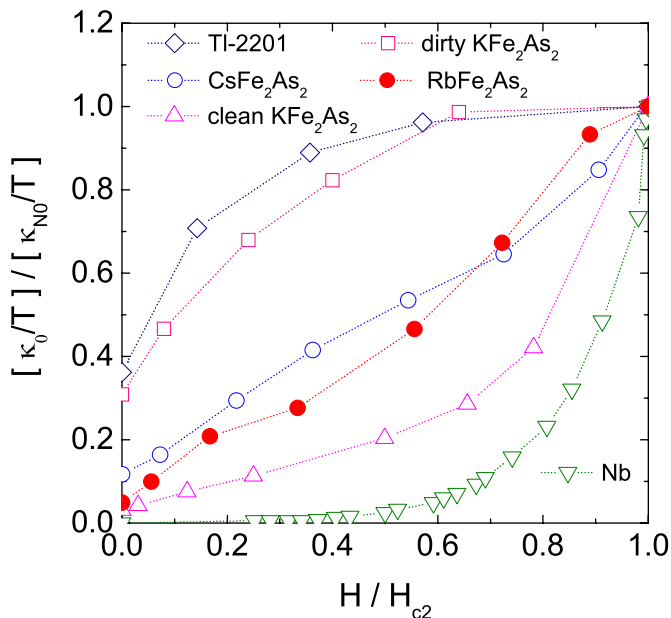


FIG. 4. (Color online). Normalized residual linear term κ_0/T of RbFe_2As_2 as a function of H/H_{c2} . For comparison, similar data are shown for the clean s -wave superconductor Nb [35], the d -wave cuprate superconductor Tl-2201 [36], the dirty and clean KFe_2As_2 [11, 17], and CsFe_2As_2 [27].

TABLE I. The superconducting transition temperature T_c , residual resistivity ρ_0 , zero-field normal-state Sommerfeld coefficient γ_N , upper critical field $H_{c2}(0)$, and residual linear term κ_0/T of the clean and dirty KFe_2As_2 , CsFe_2As_2 , and RbFe_2As_2 . These values are taken from Refs. [11, 17, 26, 27, 38–40] and this work.

	T_c (K)	ρ_0 ($\mu\Omega\text{ cm}$)	γ_N ($\frac{\text{mJ}}{\text{molK}^2}$)	$H_{c2}(0)$ (T)	κ_0/T ($\frac{\text{mW}}{\text{K}^2\text{cm}}$)
KFe_2As_2 (clean)	3.8	0.21	94	1.60	3.60
KFe_2As_2 (dirty)	2.5	3.32	91	1.25	2.27
RbFe_2As_2	2.1	1.84	127	0.97	0.65
CsFe_2As_2	1.8	1.80	184	1.40	1.27

value is slightly lower than that obtained from resistivity measurements, but it does not affect our discussion of the field dependence of κ_0/T below.

The field dependence of κ_0/T may provide more information on the superconducting gap structure [32]. In Fig. 4, we plot the normalized $\kappa_0(H)/T$ of RbFe_2As_2 together with the typical s -wave superconductor Nb [35], the d -wave cuprate superconductor $\text{Tl}_2\text{Ba}_2\text{CuO}_{6+\delta}$ (Tl-2201) [36], the dirty and clean KFe_2As_2 [11, 17], and CsFe_2As_2 [27]. For an s -wave superconductor with isotropic gap, such as Nb, κ_0/T grows exponentially with the field [35]. For the d -wave superconductor Tl-2201, κ_0/T increases roughly proportional to $H^{1/2}$ at low field [36], due to the Volovik effect [37]. From Fig. 4, the normalized $\kappa_0(H)/T$ curve of RbFe_2As_2 is very close to that of CsFe_2As_2 and lies between the dirty and clean KFe_2As_2 .

As listed in Table I, the ρ_0 of dirty and clean KFe_2As_2

differ by 15 times [11, 17], while RbFe_2As_2 and CsFe_2As_2 have comparable ρ_0 , with values lying between that of dirty and clean KFe_2As_2 . Therefore, in (K,Rb,Cs) Fe_2As_2 serial superconductors, the field dependence of κ_0/T seems to correlate with the impurity level. Although Reid *et al.* argued that the $\kappa_0(H)/T$ of clean KFe_2As_2 is a compelling evidence for d -wave gap [17], recent thermal conductivity measurements on highly hole-doped $\text{Ba}_{1-x}\text{K}_x\text{Fe}_2\text{As}_2$ single crystals support nodal s -wave gap [21]. For such a complex nodal s -wave gap structure, likely with both nodal and nodeless gaps of different magnitudes, it is hard to get a theoretical curve of $\kappa_0(H)/T$. One needs to carefully consider the effect of impurity on the behavior of $\kappa_0(H)/T$. Nevertheless, the evolution of the normalized $\kappa_0(H)/T$ suggests a common nodal gap structure in (K,Rb,Cs) Fe_2As_2 serial superconductors.

In Table I, we also list the T_c , γ_N , $H_{c2}(0)$, and κ_0/T of the (K,Rb,Cs) Fe_2As_2 serial superconductors [11, 17, 26, 27, 38–40]. Both T_c and γ_N show a systematic change with increasing the ionic radii of alkali metal. The γ_N values of RbFe_2As_2 and CsFe_2As_2 are very large among all iron-based superconductors, which reflects their abnormally large density of states or effective mass of electrons. This may be explained by recent ARPES measurement on CsFe_2As_2 single crystals, which suggests that the large separation of FeAs layers along c axis makes the system more two-dimensional and enhances the electronic correlations [41]. Neither the $H_{c2}(0)$ nor κ_0/T shows a systematic change. The $H_{c2}(0)$ of CsFe_2As_2 is abnormally high, which may also relate to its much enhanced two dimensionality and electronic correlations. As for the κ_0/T , it depends on the very details of the nodal gap, such as the slope of the gap at the node. For the accidental nodes appearing in the complex Fermi surfaces of (K,Rb,Cs) Fe_2As_2 , the κ_0/T may not necessarily manifest systematic change with the increase of the ionic radii of alkali metal.

IV. SUMMARY

In summary, we have measured the magnetization, resistivity, low-temperature specific heat and thermal conductivity of RbFe_2As_2 single crystals. A nodal superconducting gap in RbFe_2As_2 is strongly suggested by the observation of a significant residual linear term $\kappa_0/T = 0.65\text{ mW K}^{-2}\text{ cm}^{-1}$ in zero magnetic field. It is concluded that (K,Rb,Cs) Fe_2As_2 serial superconductors may have a common nodal gap structure, and the field dependence of κ_0/T seems to evolve with the impurity level.

ACKNOWLEDGEMENTS

This work is supported by the Natural Science Foundation of China, the Ministry of Science and Technology of China (National Basic Research Program No: 2012CB821402 and 2015CB921401), Program for

Professor of Special Appointment (Eastern Scholar) at
Shanghai Institutions of Higher Learning.

* E-mail: shiyan_li@fudan.edu.cn

-
- [1] Y. Kamihara, T. Watanabe, M. Hirano, and H. Hosono, *J. Am. Chem. Soc.* **130**, 3296 (2008).
- [2] X. H. Chen, T. Wu, G. Wu, R. H. Liu, H. Chen, and D. F. Fang, *Nature (London)* **453**, 761 (2008).
- [3] I. I. Mazin, D. J. Singh, M. D. Johannes, and M. H. Du, *Phys. Rev. Lett.* **101**, 057003 (2008).
- [4] H. Ding, P. Richard, K. Nakayama, K. Sugawara, T. Arakane, Y. Sekiba, A. Takayama, S. Souma, T. Sato, T. Takahashi, Z. Wang, X. Dai, Z. Fang, G. F. Chen, J. L. Luo, and N. L. Wang, *Europhys. Lett.* **83**, 47001 (2008).
- [5] P. J. Hirschfeld, M. M. Korshunov, and I. I. Mazin, *Rep. Prog. Phys.* **74**, 124508 (2011).
- [6] G. R. Stewart, *Rev. Mod. Phys.* **83**, 1589 (2011).
- [7] X. F. Wang, T. Wu, G. Wu, H. Chen, Y. L. Xie, J. J. Ying, Y. J. Yan, R. H. Liu, and X. H. Chen, *Phys. Rev. Lett.* **102**, 117005 (2009).
- [8] K. Terashima, Y. Sekiba, J. H. Bowen, K. Nakayama, T. Kawahara, T. Sato, P. Richard, Y.-M. Xu, L. J. Li, G. H. Cao, Z.-A. Xu, H. Ding, and T. Takahashi, *Proc. Natl. Acad. Sci.* **106**, 7330 (2009).
- [9] X. G. Luo, M. A. Tanatar, J.-Ph. Reid, H. Shakeripour, N. Doiron-Leyraud, N. Ni, S. L. Bud'ko, P. C. Canfield, H. Q. Luo, Z. S. Wang, H.-H. Wen, R. Prozorov, and L. Taillefer, *Phys. Rev. B* **80**, 140503(R) (2009).
- [10] M. A. Tanatar, J.-Ph. Reid, H. Shakeripour, X. G. Luo, N. Doiron-Leyraud, N. Ni, S. L. Bud'ko, P. C. Canfield, R. Prozorov, and L. Taillefer, *Phys. Rev. Lett.* **104**, 067002 (2010).
- [11] J. K. Dong, S. Y. Zhou, T. Y. Guan, H. Zhang, Y. F. Dai, X. Qiu, X. F. Wang, Y. He, X. H. Chen, and S. Y. Li, *Phys. Rev. Lett.* **104**, 087005 (2010).
- [12] K. Hashimoto, A. Serafin, S. Tonegawa, R. Katsumata, R. Okazaki, T. Saito, H. Fukazawa, Y. Kohori, K. Kihou, C. H. Lee, A. Iyo, H. Eisaki, H. Ikeda, Y. Matsuda, A. Carrington, and T. Shibauchi, *Phys. Rev. B* **82**, 014526 (2010).
- [13] Y. Nakai, T. Iye, S. Kitagawa, K. Ishida, S. Kasahara, T. Shibauchi, Y. Matsuda, and T. Terashima, *Phys. Rev. B* **81**, 020503(R) (2010).
- [14] K. Hashimoto, M. Yamashita, S. Kasahara, Y. Senshu, N. Nakata, S. Tonegawa, K. Ikada, A. Serafin, A. Carrington, T. Terashima, H. Ikeda, T. Shibauchi, and Y. Matsuda, *Phys. Rev. B* **81**, 220501(R) (2010).
- [15] Y. Zhang, Z. R. Ye, Q. Q. Ge, F. Chen, J. Jiang, M. Xu, B. P. Xie, and D. L. Feng, *Nat. Phys.* **8**, 371 (2012).
- [16] X. Qiu, S. Y. Zhou, H. Zhang, B. Y. Pan, X. C. Hong, Y. F. Dai, M. J. Eom, J. S. Kim, Z. R. Ye, Y. Zhang, D. L. Feng, and S. Y. Li, *Phys. Rev. X* **2**, 011010 (2012).
- [17] J.-Ph. Reid, M. A. Tanatar, A. Juneau-Fecteau, R. T. Gordon, de Cotret S. René, N. Doiron-Leyraud, T. Saito, H. Fukazawa, Y. Kohori, K. Kihou, C. H. Lee, A. Iyo, H. Eisaki, R. Prozorov, and Louis Taillefer, *Phys. Rev. Lett.* **109**, 087001 (2012).
- [18] F. F. Tafti, A. Juneau-Fecteau, M-è. Delage, de Cotret S. René, J.-Ph. Reid, A. F. Wang, X. G. Luo, X. H. Chen, N. Doiron-Leyraud, and Louis Taillefer, *Nat. Phys.* **9**, 349 (2013).
- [19] K. Okazaki, Y. Ota, Y. Kotani, W. Malaen, Y. Ishida, T. Shimojima, T. Kiss, S. Watanabe, C.-T. Chen, K. Kihou, C. H. Lee, A. Iyo, H. Eisaki, T. Satio, H. Fukazawa, Y. Kohori, K. Hashimoto, T. Shibauchi, Y. Matsuda, H. Ikeda, H. Miynhara, R. Arita, A. Chiainani, and S. Shin, *Science* **337**, 1314 (2012).
- [20] N. Xu, P. Richard, X. Shi, A. van Roekeghem, T. Qian, E. Razzoli, E. Rienks, G.-F. Chen, E. Ieki, K. Nakayama, T. Sato, T. Takahashi, M. Shi, and H. Ding, *Phys. Rev. B* **88**, 220508(R) (2013).
- [21] X. C. Hong, A. F. Wang, Z. Zhang, J. Pan, L. P. He, X. G. Luo, X. H. Chen, and S. Y. Li, arXiv:1401.0792.
- [22] K. Sasmal, Bing Lv, B. Lorenz, A. M. Guloy, F. Chen, Y.-Y. Xue, and C.-W. Chu, *Phys. Rev. Lett.* **101**, 107007 (2008).
- [23] Z. Bukowski, S. Weyeneth, R. Puzniak, J. Karpinski, and B. Batlogg, *Physica C* **470**, S328 (2010).
- [24] Z. Shermadini, J. Kanter, C. Baines, M. Bendele, Z. Bukowski, R. Khasanov, H.-H. Klauss, H. Luetkens, H. Maeter, G. Pascua, B. Batlogg, and A. Amato, *Phys. Rev. B* **82**, 144527 (2010).
- [25] Z. Shermadini, H. Luetkens, A. Maisuradze, R. Khasanov, Z. Bukowski, H.-H. Klauss, and A. Amato, *Phys. Rev. B* **86**, 174516 (2012).
- [26] A. F. Wang, B. Y. Pan, X. G. Luo, F. Chen, Y. J. Yan, J. J. Ying, G. J. Ye, P. Cheng, X. C. Hong, S. Y. Li, and X. H. Chen, *Phys. Rev. B* **87**, 214509 (2013).
- [27] X. C. Hong, X. L. Li, B. Y. Pan, L. P. He, A. F. Wang, X. G. Luo, X. H. Chen, and S. Y. Li, *Phys. Rev. B* **87**, 144502 (2013).
- [28] Sergey L. Bud'ko, Yong Liu, Thomas A. Lograsso, and Paul C. Canfield, *Phys. Rev. B* **86**, 224514 (2012).
- [29] S. W. Zhang, L. Ma, Y. D. Hou, J. Zhang, T.-L. Xia, G. F. Chen, J. P. Hu, G. M. Luke, and W. Yu, *Phys. Rev. B* **81**, 012503 (2010).
- [30] J. A. Woollam, P. B. Somoano, and P. O. Connor, *Phys. Rev. Lett.* **32**, 712 (1974).
- [31] C. K. Jones, J. K. Hulm, and B. S. Chandrasekhar, *Rev. Mod. Phys.* **36**, 74 (1964).
- [32] H. Shakeripour, C. Petrovic, and L. Taillefer, *New J. Phys.* **11**, 055065 (2009).
- [33] M. Sutherland, D. G. Hawthorn, R. W. Hill, F. Ronning, S. Wakimoto, H. Zhang, C. Proust, Etienne Boaknin, C. Lupien, Louis Taillefer, Rui xing Liang, D. A. Bonn, W. N. Hardy, Robert Gagnon, N. E. Hussey, T. Kimura, M. Nohara, and H. Takagi, *Phys. Rev. B* **67**, 174520 (2003).
- [34] S. Y. Li, J.-B. Bonnemaïson, A. Payeur, P. Fournier, C. H. Wang, X. H. Chen, and Louis Taillefer, *Phys. Rev. B* **77**, 134501 (2008).
- [35] J. Lowell, and J. B. Sousa, *J. Low. Temp. Phys.* **3**, 65 (1970).
- [36] C. Proust, E. Boaknin, R. W. Hill, Louis Taillefer, and A. P. Mackenzie, *Phys. Rev. Lett.* **89**, 147003 (2002).
- [37] G. E. Volovik, *JETP Lett.* **58**, 469 (1993).
- [38] M. Abdel-Hafez, S. Aswartham, S. Wurmehl, V. Grinenko, C. Hess, S.-L. Drechsler, S. Johnston, A. U. B.

- Wolter, and B. Büchner, H. Rosner, L. Boeri, Phys. Rev. B **85**, 134533 (2012).
- [39] J. S. Kim, E. G. Kim, G. R. Stewart, X. H. Chen, and X. F. Wang, Phys. Rev. B **83**, 172502 (2011).
- [40] T. Terashima, M. Kimata, M. Satsukawa, A. Harada, K. Hazama, S. Uji, H. Harima, G. F. Chen, J. L. Luo, and N. L. Wang, J. Phys. Soc. Jpn. **78**, 063702 (2009).
- [41] S. Kong, D. Y. Liu, S. T. Cui, S. L. Ju, A. F. Wang, X. G. Luo, L. J. Zou, X. H. Chen, G. B. Zhang, and Z. Sun, arXiv:1409.2300.